Depicting Beyond Scores: Advancing Image Quality Assessment through Multi-modal Language Models

Zhiyuan You[1,2*], Zheyuan Li[2*], Jinjin Gu[3,4*], Zhenfei Yin[3,4], Tianfan Xue[1,4†], Chao Dong[2,4†]
[1]The Chinese University of Hong Kong,
[2]Shenzhen Institute of Advanced Technology, Chinese Academy of Sciences,
[3]University of Sydney, [4]Shanghai AI Laboratory
zhiyuanyou@foxmail.com zheyuanli884886@gmail.com jinjin.gu@sydney.edu.au
zyin7056@uni.sydney.edu.au tfxue@ie.cuhk.edu.hk chao.dong@siat.ac.cn

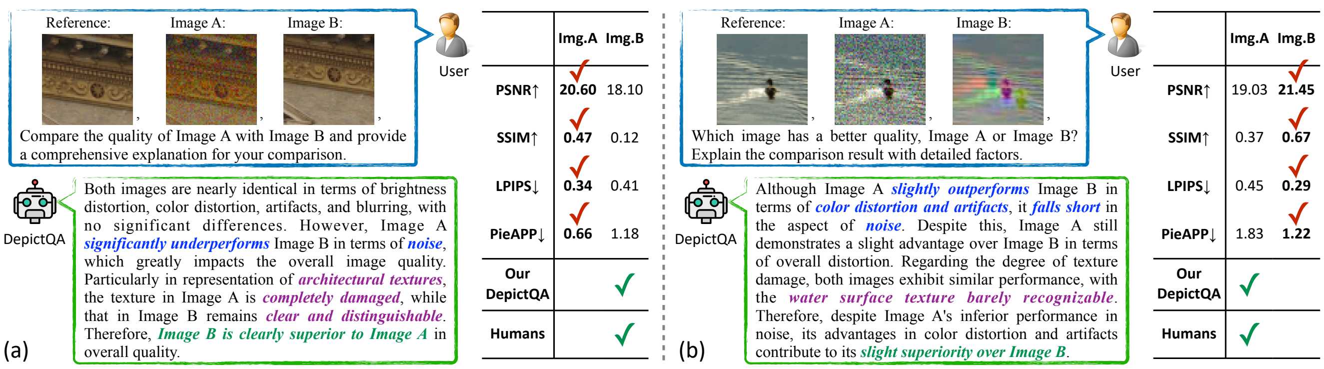

Figure 1. **Comparison** between our Depicted image Quality Assessment method (DepictQA) and score-based Image Quality Assessment (IQA) methods, including PSNR, SSIM [49], LPIPS [55], and PieAPP [38]. Score-based IQA methods only provide numerical scores devoid of reasoning and justification. They disagree with human judgments in complex scenarios when **(a)** images are misaligned and **(b)** both images suffer from severe distortions. In contrast, DepictQA first identifies the distortions of images, then weighs the influences of different distortions to the texture damages, and finally obtains the comparison results that are better aligned with human judgments.

Abstract

*We introduce a **Depict**ed image **Q**uality **A**ssessment method (DepictQA), overcoming the constraints of traditional score-based approaches. DepictQA leverages Multi-modal Large Language Models (MLLMs), allowing for detailed, language-based, human-like evaluation of image quality. Unlike conventional Image Quality Assessment (IQA) methods relying on scores, DepictQA interprets image content and distortions descriptively and comparatively, aligning closely with humans' reasoning process. To build the DepictQA model, we establish a hierarchical task framework, and collect a multi-modal IQA training dataset, named M-BAPPS. To navigate the challenges in limited training data and processing multiple images, we propose to use multi-source training data and specialized image tags. Our DepictQA demonstrates a better performance than score-based methods on the BAPPS benchmark. Moreover, compared with general MLLMs, our DepictQA can generate more accurate reasoning descriptive languages. Our research indicates that language-based IQA methods have the potential to be customized for individual preferences. Datasets and codes will be released publicly.*

1. Introduction

Image Quality Assessment (IQA) is an important and challenging topic of low-level vision research. IQA aims to measure and compare the quality of images, expecting the final results to be aligned with human judgments. Existing IQA methods [15, 38, 49, 55] mainly output the quality or similarity scores, which have apparent shortcomings. First, image quality is affected by different factors that cannot be effectively expressed by a simple score, *e.g.*, noise, color distortion, and artifacts in Fig. 1a and 1b. Second, the reasoning process by human evaluators cannot be well modeled by current IQA methods. For example, in Fig. 1b, humans first identify the image distortions (*i.e.*, noise in Image

* Contribute Equally. † Corresponding Author.
Project Page: https://zhiyuanyou.github.io/DepictQA/.

A, color distortion and artifacts in Image B), then weigh the impacts of these distortions on overall visual quality (color distortion and artifacts in Image B are worse than noise in Image A), and finally conclude that Image A is better than Image B. On the contrary, existing IQA methods simply compare the quality scores of these two images.

To better align with human evaluators, we explore a new paradigm for IQA, named **Depict**ed image **Q**uality **A**ssessment (DepictQA). Inspired by recent Large Language Models (LLMs) [32, 45] and multi-modal technologies [24, 62], we believe that language is the key to solving the above problems. As shown in Fig. 1, DepictQA takes both images and a question as inputs, then outputs a paragraph that describes the quality of images from multiple aspects. Furthermore, empowered by the reasoning capability of LLMs, DepictQA can weigh the importance of each distortion and make the final judgment. For instance, in Fig. 1a, DepictQA finds that "the texture in Image A is completely damaged" while "Image B remains clear and distinguishable", thus concludes "Image B is clearly superior to Image A". Learning this kind of reasoning makes DepictQA better at aligning human judgments than existing methods in complex scenarios like misalignment (Fig. 1a) and multiple distortions (Fig. 1b). Meanwhile, these descriptive outputs can be naturally understood by humans, greatly improving the interpretability.

To integrate language into IQA, we establish a hierarchy of tasks for DepictQA, inspired by human evaluation. Humans first perceive the distortions of the image, then use this information to determine the image quality. Also, it is easier for humans to compare the difference between two images in a single dimension (*e.g*., color distortion) than quantitatively evaluate the overall quality of an image or the similarity between two images, as verified by [36–38]. Based on this intuition, DepictQA does not produce "scores", but describes the image quality and compares two images. Specifically, we break DepictQA problem into a hierarchy of three tasks (detailed in Fig. 2): (1) Quality Description, (2) Quality Comparison, and (3) Comparison Reasoning. These designs can reflect humans' evaluation process.

To train the proposed DepictQA, we further construct a multi-modal IQA dataset named M-BAPPS by collecting text descriptions based on the existing BAPPS IQA dataset [55]. Our M-BAPPS dataset contains 5,104 detailed high-quality text descriptions and 115,646 brief descriptions. For high-quality texts, we first collect the quality-related information through a carefully designed questionnaire (details shown in Fig. 2a and 2c), the results of which are further converted into a descriptive paragraph using GPT-4 [32]. To further increase the size of the training set, we also augment the dataset with brief descriptions. Specifically, we convert the existing quality comparison label in BAPPS into a brief description using pre-generated templated texts, such as "Image A maintains a distinct advantage in terms of image quality over Image B".

With the dataset mentioned above, we resort to Multi-modal Large Language Models (MLLMs) [18, 24, 62] to bridge the gap between images and descriptive texts. However, directly applying existing MLLMs to our DepictQA faces two challenges. First, there are only limited images with high-quality descriptions, preventing the model from robustly correlating images and text descriptions. In this aspect, we present a multi-source training approach to increase the size of training data. Specifically, two additional sources are used. One is images with only brief templated texts, as mentioned above. The other is external quality-unrelated content description data, the Detailed Description dataset in [53], which contains 48,734 image-text pairs. Although these two datasets are not directly designed for the descriptive reasoning ability, we find that the former one can help bridge images and texts in quality-related tasks, while the latter one can serve as regularization. Second, many MLLMs have difficulty in distinguishing multiple images, but our setup requires two or more images. We solve this problem by employing specialized tags for different images, instead of a unified tag for all images. Empirical results demonstrate that these approaches effectively mitigate the two challenges and bring a better DepictQA model.

At last, we conduct several experiments to prove the effectiveness of DepictQA. Firstly, DepictQA achieves the state-of-the-art performance on the BAPPS benchmark, well aligned with human judgments. Additionally, DepictQA can describe the distortions and texture damages in images and explain the reasoning process when comparing two images, thus generating more accurate descriptions compared with general-purpose MLLMs. Even compared with notably GPT-4V [33], DepictQA has significantly better comparison ability and comparable reasoning ability. Our investigation also shows that DepictQA has the potential to integrate individual preferences into the evaluation process. These results attest to the superiority of the proposed DepictQA, and the research potential of Multi-modal IQA tasks.

2. Related Works

Score-based IQA methods. Most existing IQA methods rely on scores to assess image quality. They can be categorized into *full-reference* and *non-reference* methods. (1) Full-reference methods assess image quality by computing the similarity score between a distorted image and a high-quality reference image. Traditional methods rely on human-designed metrics like structural similarity [49], image information [41], phase congruency with gradient magnitude [54], *etc*. Learning-based methods aim to align with human assessment through data-driven training. LPIPS [55] shows that the learned features can effectively function as a perceptual metric, exhibiting high consistency with human judgments. In alignment with advancements in the deep-learning community, data-driven approaches [4, 6, 10, 11, 13, 38, 52, 61] have similarly spurred innovations in IQA. (2) Non-reference methods evaluate the quality of a distorted image without a reference image. Traditional methods [26–31, 40, 44] primarily calculate quality scores based on human-designed natural image statistics. Deep-learning-based methods [19, 20, 25, 35, 42, 60, 63] replace hand-crafted statistics by learning quality priors from extensive data. Recent works further enhance the performance by introducing graph representation [43], CLIP pre-training [48], continual learning [57], multitask learning [58], and so on. However, score-based IQA methods exhibit inherent limitations, particularly the inability to reflect the intricate analyses and weights of multiple aspects, as discussed in Sec. 1.

Multi-modal Large Language Models (MLLMs) incorporate other modalities (especially visions) into LLMs by leveraging the emergent ability of LLMs [32]. Early efforts [7, 47] primarily focus on data-efficient fine-tuning, while recent advancements [12, 18] build end-to-end trainable frameworks on web-scale multi-modal corpora. Various approaches choose to train different modules, *e.g.*, the vision-to-text alignment modules [23, 62], the medium-gated layers [1], and the core LLMs [24, 51]. Recent studies emphasize integrating the intermediate features [14, 22, 56], improving in-context learning [59], and establishing comprehensive multi-modal benchmarks [53], *etc*. Recently, GPT-4V [33] has showcased remarkable capabilities in general visual understanding. However, we demonstrate in Sec. 5.3 that general MLLMs are not good at IQA tasks.

MLLMs for IQA. Q-Bench [50] introduces a comprehensive validation dataset to assess existing MLLMs in low-level perception and understanding tasks. Our work distinguishes itself from Q-Bench in two key aspects. First, in the task definition, our focus lies on quality comparison regarding distortions and texture damages across multiple images, whereas Q-Bench primarily centers on low-level descriptions within individual images. Second, Q-Bench evaluates existing general MLLMs with a newly constructed validation set, whereas we develop a specific MLLM for IQA that substantially outperforms existing general MLLMs.

3. DepictQA Task and Dataset

3.1. Task Description

Before introducing our method, we need to rethink the paradigm of IQA. To reflect the human process of assessing image quality, we intend to apply language as a powerful interactive and logical tool. Intuitively, the proposed DepictQA should have the following abilities.

First, DepictQA needs to **identify the distortions and texture damages** (Fig. 2a). Humans begin assessing image quality by identifying distortions and texture damages, as this is the basis for any subsequent assessment.

Second, DepictQA is required to **compare distorted images** like Fig. 2b rather than just calculate scores for individual images. Quantifying image quality has drawbacks, as the information from a single score is quite limited. It has also been verified that humans tend to make a biased quality assessment on a single image, but be more consistent and reliable on comparing two images [15, 16, 37].

Third, DepictQA should additionally **weigh and judge multiple aspects** that affect image quality. Humans consider many factors when making the image quality comparison. For example, when comparing an underexposed image and a blurry image in Fig. 2c, one may need to consider the actual impacts of these two distortions on the texture representation, and weigh among these considerations. DepictQA should mimic this weighing ability, which distinguishes DepictQA from previous IQA methods.

Based on the above discussion, as described in Fig. 2, we design a hierarchical task paradigm for DepictQA, progressively guiding the model to obtain the above abilities:

- *Task–1: Quality Description*. Based on the provided reference image and a distorted image, describe the distortions and texture damages in the distorted image, and comment on the overall quality of the distorted image.
- *Task–2: Quality Comparison*. Based on the provided reference image and two different distorted images, determine which distorted image has a better quality.
- *Task–3: Comparison Reasoning*. Based on the comparison result, describe the distortions and texture damages of the two distorted images, make inferences, and weigh the pros and cons to justify its judgment on image quality.

3.2. Dataset Construction

Data serves as the key factor for training MLLMs. We follow the scheme of supervised fine-tuning [24, 53] to train DepictQA. Supervised fine-tuning requires collecting {images, question, response} data pairs, where "images" are the ones to be evaluated, "question" describes the task, and "response" is the reference answer. In this section, we describe in detail our selection of images and the collection of questions and responses for the three tasks.

Image collection for the IQA dataset consists of two aspects, one is the selection of reference images, and the other is the collection of distorted images. Existing works usually collect a large number of distorted images on a small number of reference images [15, 16, 37, 38]. However, the semantic richness of the training images are also very important. In our work, we collect reference images and their corresponding distorted images from the BAPPS dataset [55]. BAPPS dataset contains 197k highly diverse samples, meeting the diversity requirements of DepictQA training. For each sample, there is a reference image and its two distorted versions, as given in Fig. 2b and 2c. BAPPS dataset also

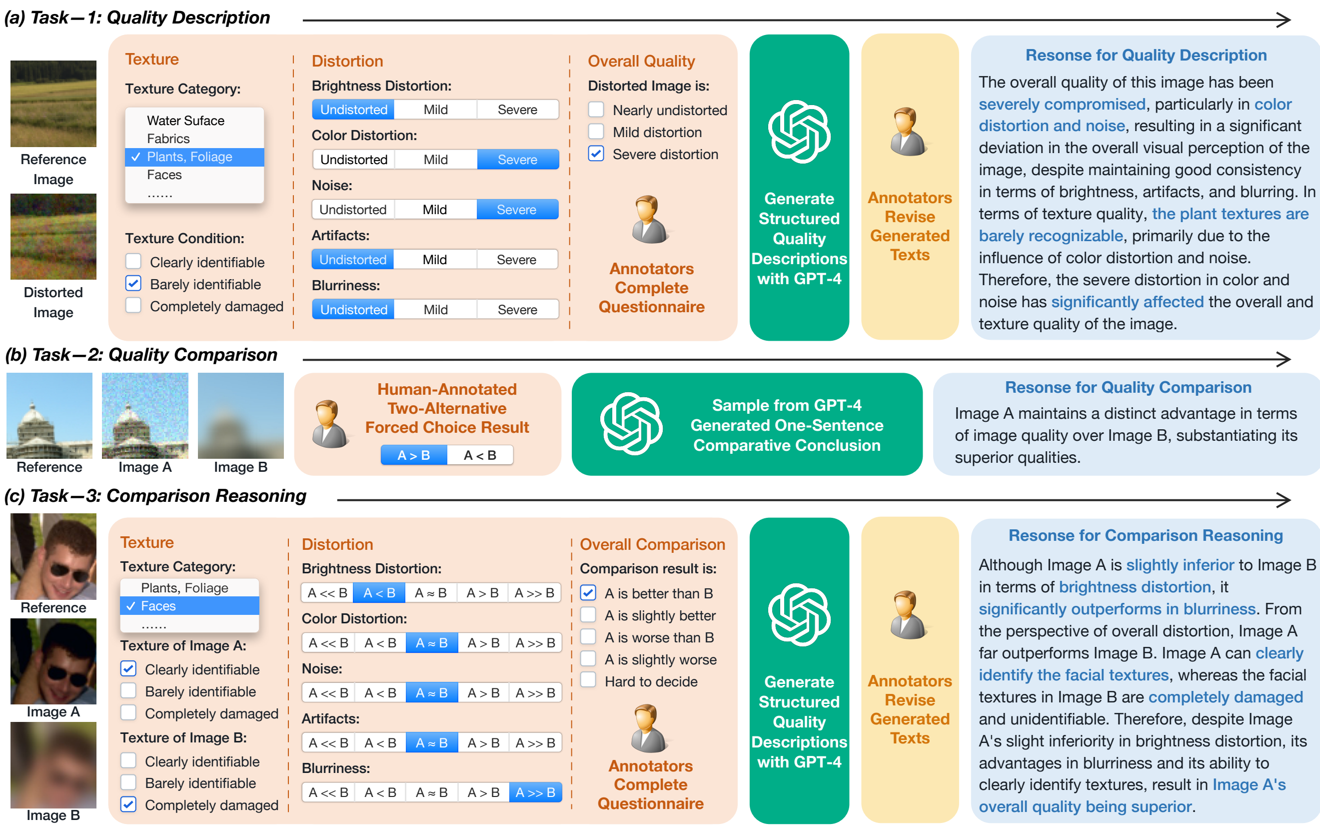

Figure 2. **Collection of the responses in our M-BAPPS dataset**. We first carefully design a questionnaire to collect quality-related information. We then employ the GPT-4 [32] to convert our annotated questionnaire results into natural language. Finally, the outputs of GPT-4 are modified and improved by the annotators to correct errors, eliminate ambiguities, and supplement important information.

provides human annotations, indicating which distorted image is more similar to the reference one, *i.e.*, has better perceptual quality. These annotations can be used to build our dataset and validate our newly annotated data.

Question collection. For each task, users may express similar questions in different sentences, like the two questions in Fig. 1. To encourage the robustness of DepictQA to users' questions, for each task, we first leverage GPT-4 to generate 30 questions. We then manually remove ambiguous and duplicate questions and modify inaccurate questions to form a set of 10 questions (see *Appendix*). During training and testing, we randomly sample a question from the question set to construct the data pair.

Response collection. A straightforward method to collecting high-quality texts requires manually writing the training texts [34, 46]. However, when annotators are inexperienced or tired, human-written texts can lead to huge biases and uneven quality. In this work, we use advanced LLMs to assist annotators in generating structured training texts, as illustrated in Fig. 2. We first collect the information that we want the texts to describe through a carefully designed questionnaire. Answering questions greatly reduces the possibility of ambiguity among annotators and ensures that the information is structured. We then use GPT-4 to convert our annotated questionnaire results into natural language. Finally, the outputs of GPT-4 are modified and improved by the annotators to correct errors, eliminate ambiguities, and add important information. This process greatly reduces the difficulty of collecting training texts and improves the quality of the training texts. Next, we introduce the details of the questionnaire for different tasks.

Task–1: Quality Description. A distorted image and its reference image are shown to annotators. Fig. 2a shows our questionnaire with three parts: texture, distortion, and overall quality. For the texture part, annotators are asked to select the one that best matches the image from a list containing 11 typical texture types, including object edges, bricks, fabrics, plants or foliage, architectures, artificial strips, hairs or furs, faces, sky or clouds, stones or ground, and water surface. These 11 types are selected based on the existing IQA [16] and texture recognition [2] research. Additionally, annotators are asked to indicate whether the texture is "clearly identifiable", "barely identifiable", or "completely damaged". Regarding the distortion part, we ask annotators to summarize from the following five aspects: "brightness", "color", "noise", "artifacts", and "blurriness". For each distortion, we use three levels for evaluation: "undistorted", "mild", and "severe". This can express most distortions that

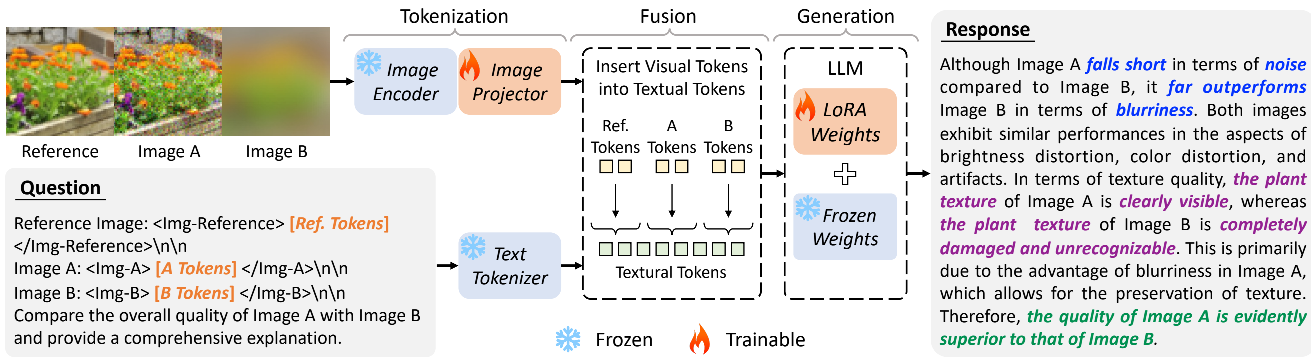

Figure 3. **Framework of our DepictQA**. A frozen pre-trained image encoder is employed to encode images to visual tokens, followed by a trainable image projector to project visual tokens to textual space. The question texts are tokenized by a text tokenizer. Visual tokens and textual tokens are then fused and jointly processed by an LLM, fine-tuned through the LoRA technique [17]. As exemplified by Comparison Reasoning, our model is capable of producing comprehensive and informative explanations for image quality comparisons.

appear in images. Finally, annotators need to comment on the overall quality of the image into three levels: "nearly undistorted", "mild distortion", and "severe distortion".

Task–2: Quality Comparison. BAPPS dataset already includes binary comparison labels (*i.e.*, Image A or Image B is better) for all image pairs. To convert these comparison labels into textural responses, we first build a response pool using GPT-4, including 20 generated sentences for "Image A is better" and another 20 for "Image B is better". Then, for each comparison label, we randomly sample one response from the pool, as depicted in Fig. 2b.

Task–3: Comparison Reasoning. As shown in Fig. 2c, annotators are given two distorted images and the reference image. The annotation pipeline is similar to Task–1. Annotators compare two distorted images from the five kinds of distortions and the overall distortion using five options: "superior" ($>>$), "slightly superior" ($>$), "roughly equal" ($\approx$), "slightly inferior" ($<$), and 'inferior" ($<<$).

Dataset statistics. The statistics of our dataset are presented in Tab. 1 (more in *Appendix*). Our dataset comprises 5,104 detailed high-quality samples (Task–1 and Task–3), along with 115,646 brief templated samples (training set of Task–2). Each training sample is individually annotated by one annotator. In the validation set, samples are annotated by two annotators only if they reach a consensus. As a means of verification, the annotated "Overall Comparison" judgments in Task–3 exhibit a quite high consistency rate of 84.3% with the ground-truth judgments in the BAPPS dataset. For brevity, the three tasks will be shortened to *description*, *comparison*, and *reasoning* in the following.

Table 1. **Statistics of our M-BAPPS dataset**. The validation set of Task–2 is the same as the "Traditional" and "CNN" categories (two sets of distortions) in BAPPS's validation set [55].

	# Task–1 Quality Description	# Task–2 Quality Comparison	# Task–3 Comparison Reasoning
Train	1,115	115,646	3,739
Validation	50	9, 440	200
Total	1,165	125,086	3,939

4. DepictQA Framework

4.1. Model Architecture

Fig. 3 shows the workflow of our DepictQA. DepictQA takes images and a quality-related question as inputs, and generate descriptive texts as response. In *comparison* or *reasoning* tasks, there are three input images: a reference image and Image A and B. In *description* task, there are two input images: a reference image and a distorted image. The input images and question are first tokenized, then fused, finally processed by the LLM for response generation.

Tokenizing input images and question. As shown in Fig. 3, we employ a frozen CLIP pre-trained ViT-L/14 [39] as the image encoder to represent the input images as visual tokens. Then, the question texts are tokenized to textual tokens by SentencePiece tokenizer [21]. The visual tokens cannot be directly processed by the LLM due to different embedding spaces, so we use a trainable image projector to map visual tokens into the textual space as in [24, 62].

Token fusion. We insert the visual tokens into predefined positions within the textual tokens, *i.e.*, [*Ref. Tokens*], [*A Tokens*], [*B Tokens*] in the input question in Fig. 3.

Response generation using LLM. The fused tokens are fed into LLM to generate the final response. We use Vicuna-v1.5-7B [8] as the LLM. Pre-trained LLMs do not work well on IQA tasks, and need to be fine-tuned on our dataset. However, complete LLM fine-tuning is resource-intensive and data-hungry, requiring tens of thousands of high-quality human-written texts [34]. To get around of data shortage issue, we resort to LoRA [17], an efficient LLM fine-tuning technique, which selectively adjusts only a small set of parameters in the LLM. Following [17, 53], we apply LoRA to fine-tune the projection layers in all self-attention modules.

Unique tag to distinguish multiple images. Existing

MLLMs [24, 62] are primarily designed to handle a single input image. They insert the visual tokens between the start (*e.g.*, `<Img>`) and end (*e.g.*, `</Img>`) tags. A simple extension to multi-image input is using textual cues to distinguish images, *e.g.*, adding "Reference Image:", "Image A:", and "Image B:" before visual tokens. However, this simple extension sometimes fails to distinguish images, probably because the proportion of these short textual cues in the full texts is too small. To mitigate this, motivated by [59], we adpot the unique tag for each image. In *comparison* and *reasoning* tasks, we select `<Img-Reference>`, `<Img-A>`, and `<Img-B>` as start tags, adhering to the HTML rule by adding a trailing slash ("/") in the end tags. In *description* task, the reference image retains the same tags, while the distorted image employs the original tags, `<Img></Img>`.

4.2. Training Scheme

Multi-source training data. As stated in Sec. 1, our training images come from three sets: (1) 115,646 brief templated data of Task–2 (*comparison*), (2) 4,854 high-quality data of Task–1 (*description*) and Task–3 (*reasoning*), which are duplicated by 10 times to increase the training weights, and (3) 48,734 content description data (Detailed Description dataset in [53]), which are unrelated to IQA. The abundant templated data principally bridge images and descriptive texts in quality-related tasks. The limited yet high-quality data foster the model's descriptive and reasoning skills. The IQA-unrelated content description data can serve as regularization, given the limited text diversity of our IQA data for an MLLM. Experimental results in Tab. 5 prove the effectiveness of the three sources of training data.

Training objective. Following existing works [5, 24, 53], the training objective of DepictQA is the next token prediction loss: a cross-entropy loss between predicted and ground-truth next tokens. Note that only the tokens within the responses contribute to the loss computation. Also, only the image projection layer and LoRA parameters are optimized, comprising a mere 0.25% of the total parameters.

5. Experiments

This section discusses experimental setups and results. In our experiments, we set the LoRA rank to 16. The image size in BAPPS dataset [55] is 64×64, and we zero-pad it to 70×70, then encode it into 25 tokens. DepictQA is trained for 3 epochs on 4 GPUs (NVIDIA RTX A100 40G) with batch size 64. Adam optimizer with $(\beta_1, \beta_2) = (0.9, 0.95)$, weight decay 0.001, and learning rate 0.0005 is used for training. The total training time is around 10 hours.

5.1. Metrics

Unlike traditional score-based IQA, evaluating the descriptive textual results of IQA is not trivial. Therefore, we adopt three different metrics for comprehensive evaluation.

Accuracy. For *comparison* task, we employ the accuracy metric. Our model produces diverse textual outputs, necessitating transformation to bi-classification results (*i.e.*, Image A or B is better) for accuracy calculation, which is achieved through GPT-3.5. For users without GPT-3.5 access, we offer a pre-trained BERT [9] for classification, with a high consistency level of 97.5% with GPT-3.5.

GPT4-score. For *description* and *reasoning* tasks, following [8, 24], we utilize the GPT4-score for assessment. Specifically, we provide GPT-4 with all information in the human-labeled questionnaire as context. Then, we give GPT-4 both the model-generated response and the corresponding ground truth response. Based on the context, GPT-4 evaluates the helpfulness, relevance, accuracy, and level of detail of these two responses, and gives an overall score on a scale of 0 to 10, where a higher score indicates better quality. Finally, the relative score with regard to the ground truth response is reported as the GPT4-score.

Reasonable-rate by human evaluators. We observe that the GPT4-score exhibits excessive confidence in low-quality responses. In some cases, a fully wrong response even receives a GPT4-score over 60% (see *Appendix*). Consequently, for a more comprehensive evaluation, given both the images and responses, human evaluators label each response as reasonable or unreasonable. A reasonable response should adhere to three criteria: indicating major distortions, no severe mistakes, and logical self-consistency, which are detailed in *Appendix*. The reasonable-rate serves as another metric to assess description and reasoning ability.

5.2. Comparison with Score-based IQA Methods

To demonstrate the effectiveness of DepictQA, we compare it with score-based IQA methods on the validation set of *comparison* task (Task–2), which is the same as the "Traditional" and "CNN" categories (two sets of distortions) in BAPPS's validation set. We evaluate four traditional IQA methods including PSNR, SSIM [49], VIF [41], FSIM [54], and four deep-learning-based IQA methods including DeepIQA [3], PieAPP [38], LPIPS [55], and DISTS [10]. The results of PSNR, SSIM, and LPIPS are borrowed from [55], and the results of VIF, FSIM, DeepIQA, PieAPP, and DISTS are borrowed from [10].

Quantitative results of quality comparison on BAPPS are depicted in Tab. 2. Our DepictQA surpasses the best traditional method, FSIM, by a large margin ($\sim$10%). We also outperform the best deep-learning-based competitors, LPIPS and DISTS. Unlike high-level perception tasks where multi-modal approaches usually lag behind single-modal methods [53], we show that multi-modal IQA methods can surpass score-based counterparts. Nevertheless, the quantitative comparison is not the key issue, we pay more attention to the description and reasoning abilities.

Table 2. **Quantitative results of quality comparison task** with accuracy metric on BAPPS benchmark [55]. Our DepictQA achieves the state-of-the-art performance.

Type	Method	Distortion Category Traditional	CNN	Average
Oracle	Human	80.8	84.4	82.6
Traditional	PSNR	59.9	77.8	68.9
	SSIM [49]	60.3	79.1	69.7
	VIF [41]	55.6	74.4	65.0
	FSIM [54]	62.7	79.4	71.0
Learning	DeepIQA [3]	70.3	79.4	74.8
	PieAPP [38]	72.7	77.0	74.6
	LPIPS [55]	76.0	**82.8**	79.4
	DISTS [10]	<u>77.2</u>	82.2	<u>79.7</u>
DepictQA (Ours)		**78.4**	<u>82.7</u>	**80.6**

Table 3. **Performance comparison of DepictQA and general MLLMs**. All LLMs have 7B parameters. The comparison ability is evaluated by accuracy. Since general MLLMs can produce responses without explicit comparison results, accuracy is reported with these responses included / excluded. The description and reasoning abilities are assessed using reasonable-rate / GPT4-score. Obviously, general MLLMs are not capable of IQA tasks.

Method	LLM (7B)	Description	Comparison	Reasoning
LLaVA-v1 [24]	LLaMA-2-chat	fail	fail	fail
LLaVA-v1.5 [24]	Vicuna-v1.5	18.0 / 65.8	43.0 / 50.6	7.0 / 63.9
MiniGPT4 [62]	Vicuna-v0	16.0 / 49.9	38.0 / 46.3	1.0 / 42.4
MiniGPT4 [62]	LLaMA-2-chat	fail	fail	fail
LAMM [53]	Vicuna-v0	12.0 / 62.5	53.0 / 55.8	4.0 / 58.1
LAMM [53]	LLaMA-2-chat	8.0 / 57.4	44.0 / 48.9	5.0 / 52.4
DepictQA (ours)	Vicuna-v1.5	**64.0 / 76.2**	**82.0**	**53.0 / 76.4**

5.3. Comparison with General Multi-modal LLMs

We further compare DepictQA with general Multi-modal LLMs (MLLMs) on the validation sets of *description* (Task–1) and *reasoning* (Task–3) tasks. We also transform the reasoning responses to bi-classification results to calculate the comparison accuracy. We choose three MLLMs as baselines: LLaVA [24], MiniGPT4 [62], and LAMM [53]. The model weights are obtained from their official GitHub repositories. We provide explicit and comprehensive task instructions to inform the MLLMs of the task definition.

Quantitative results are illustrated in Tab. 3. LLaVA-v1 and MiniGPT4 (LLaMA-2-chat) fail in IQA tasks, yielding either nearly identical results or irrelevant results across most samples. Other general MLLMs also exhibit poor performance, indicating their inadequacy for IQA tasks. However, after fine-tuning on our M-BAPPS dataset, our DepictQA achieves significantly improved performance.

Qualitative results. Three qualitative results of *reasoning* task are depicted in Fig. 1 and Fig. 3. More qualitative results and failure cases of *description*, *comparison*, and *reasoning* tasks are illustrated in *Appendix*.

Table 4. **Comparison of DepictQA and GPT-4V [33]**. The comparison ability is evaluated by accuracy, while the reasoning ability is evaluated by reasonable-rate / GPT4-score.

Method	Comparison	Reasoning
GPT-4V [33]	65.0	**52.0 / 106.4**
DepictQA (ours)	**90.0**	**53.0** / 77.6

5.4. Comparison with GPT-4V

We compare DepictQA with GPT-4V [33] on the first 100 samples in the validation set of Task–3 (*reasoning*). We request GPT-4V to complete both *comparison* and *reasoning* tasks. GPT-4V is given detailed instructions and two human-labeled examples for task description. As shown in Tab. 4, our DepictQA and GPT-4V have mutual advantages and disadvantages. The GPT4-score of GPT-4V is quite high, even higher than human-annotated responses (>100%), because of the linguistic fluency and detailed description of image contents. However, we achieve comparable performance at the human-evaluated reasonable-rate. Moreover, the quality comparison ability of DepictQA is significantly better than GPT-4V. Note that GPT-4V is close-source and expensive to access, thus developing an effective MLLM for IQA is worthwhile. See *Appendix* for qualitative results and failure cases of GPT-4V.

5.5. Ablation Studies

In this section, we conduct extensive ablation studies to verify the effectiveness of our methodologies.

Effects of multi-source training data are detailed in Tab. 5. (1) Inclusion of Task-2 data (*comparison*) remarkably improves comparison accuracy (#2 *vs*. #4). Even though these texts are brief and templated, the abundant samples still help better bridge the images and texts in quality-related tasks. (2) As evidenced by #1 *vs*. #4 and #3 *vs*. #5, Task-3 data (*reasoning*) are necessary for a robust reasoning ability. Examination of #4 against #5 indicates that Task-1 data (*description*) boost both comparison and reasoning metrics, mainly by helping identify distortions. Therefore, the high-quality texts of Task–1 and Task–3 are necessary for DepictQA to depict the image quality with language. (3) Integrating content description data advances the performance (#5 *vs*. #6) by serving as regularization in light of M-BAPPS's limited text variety for an MLLM. Additionally, the content description data also helps enrich the text diversity, as shown in *Appendix*.

Unique tag effectively mitigates the confusion problem, detailed in Fig. 4. Confusion occurs when distortions in one image are mistakenly attributed to another. To quantify this, we manually review 50 responses and compute the confusion rate. With the unified tag, the model needs to distinguish images through textual hinds, as stated in Sec. 4.1,

Table 5. **Ablation studies of multi-source training data**. "Content" means the content description data. The comparison ability is assessed by accuracy within Traditional / CNN categories. The reasoning ability is evaluated by reasonable-rate / GPT4-score.

#	Training Data				Comparison	Reasoning
	Task–2	Task–1	Task–3	Content		
1	✓				77.2 / 81.4	N/A
2			✓		66.4 / 65.4	31.0 / 74.2
3	✓	✓			77.4 / 81.9	N/A
4	✓		✓		77.6 / 80.6	41.0 / 74.3
5	✓	✓	✓		78.1 / 82.1	45.0 / **77.2**
6	✓	✓	✓	✓	**78.4 / 82.7**	**53.0** / 76.4

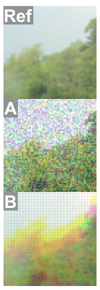

Unified Tag: *<Img>* for all three images

Response: …Image A *underperforms* Image B in terms of *color distortion*. However, Image A *excels in noise control*, clearly outperforming Image B…

Unique Tag: *<Img-Reference>*, *<Img-A>*, & *<Img-B>*

Response: …Although Image A *slightly outperforms* in terms of *color distortion*, it is markedly *inferior to* Image B in the aspect of *noise*…

	Unified Tag	Unique Tag
Confusion Rate / %	24.0	12.0

Figure 4. **Unique tag alleviates the confusion problem** using clearer instructions. The confusion rate drops dramatically.

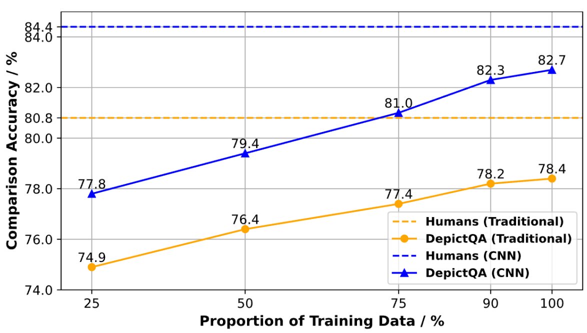

Figure 5. **The comparison performance gradually increases** with the size of training data increasing.

leading to a 24% confusion rate. Adding a unique tag for each image significantly reduces the confusion rate to 12%.

The size of training data is studied in Fig. 5. As the size of training data increases, the comparison performance gradually increases. Thus the quantity of the training data still plays a key role in the MLLM-based method.

LLMs and the initialization methods are studied in Tab. 6. For random initialization, we retrain the image projector and LoRA parameters from scratch. For high-level initialization, trainable parameters are pre-trained on high-level perception tasks (*e.g.*, detection). (1) Results from #1, #3, and #5 show that with random initialization, the effects of changing the LLM are negligible. (2) For advanced LLMs like Vicuna-v1.5 or LLaMA-2-chat, pre-training on high-level perceptual tasks (#4 and #6) markedly degrades the performance. These models' responses are more likely to describe content rather than assess quality. Hence, we suspect that for advanced LLMs, the distance between the optimal parameters of high-level perception tasks and IQA tasks is substantial. This leads to a convergence at a local optimal proximal to the pre-trained weights.

Table 6. **Ablation studies *w.r.t.* LLMs and the initialization methods**. "High-level" means the trainable parameters are pre-trained on high-level perception tasks (*e.g.*, classification and detection). The comparison ability is evaluated by accuracy within Traditional / CNN categories. For advanced LLMs, pre-training on high-level perceptual tasks markedly degrades performance.

#	LLM	Initialization	Comparison
1	Vicuna-v0-7B	Random	**78.3 / 82.4**
2	Vicuna-v0-7B	High-level	78.1 / 82.1
3	Vicuna-v1.5-7B	Random	**78.4 / 82.7**
4	Vicuna-v1.5-7B	High-level	70.6 / 73.1
5	LLaMA-2-chat-7B	Random	**78.2 / 82.7**
6	LLaMA-2-chat-7B	High-level	63.3 / 63.7

Regular Instructions

Question: Compare the quality of Image A with Image B…

Response: …Although Image B is slightly superior in handling noise, due to the advantage of Image A in color distortion, the quality of ***Image A is superior to that of Image B***…

Customized Instructions

Question: Compare the quality of Image A with Image B… ***I cannot tolerate any noise, consider noise as the most important aspect***.

Response: …Despite Image A's superior color performance, the influence of noise results in its overall quality and texture quality being ***slightly inferior to Image B***…

Figure 6. **DepictQA has the potential to be a customized IQA tool** by incorporating human preferences into instructions.

6. Extension and Limitations

Extension. Given various instructions, DepictQA has the potential to be a customized IQA tool. To demonstrate this potential, as shown in Fig. 6, we append the specific human preference (*e.g.*, cannot tolerate any noise) to the instructions, DepictQA adapts its comparison results accordingly. How to better induce this ability is our future work.

Limitations. In this preliminary attempt, we demonstrate the possibility of depicting image quality with MLLMs. There is still a long way to go for real-world application. (1) The amount and coverage of data are not sufficient, limiting the generalization to real-world images. (2) The performance in *description* and *reasoning* tasks is not satisfying, particularly in human-evaluated reasonable-rate. (3) The distortion types can be more than five, even not pre-defined. Also, more fine-grained comparisons focusing on local details are preferred. (4) Finally, whether MLLM-based IQA methods can take the place of score-based ones is still an open question. These belong to our future works.

7. Conclusion

We propose DepictQA, employing MLLMs for descriptive and human-like IQA. DepictQA differs from score-based methods by describing and comparing image distortions and texture damages with languages, well aligned with the human evaluation process. For DepictQA development, we create a hierarchical task paradigm and gather a multi-modal IQA dataset. To address issues in limited data and multiple image processing, we employ multi-source data and specific image tags. DepictQA surpasses score-based approaches in the BAPPS benchmark. Compared to general MLLMs, DepictQA outputs more precise description and reasoning results. Our work also reveals the adaptability of MLLM-based IQA methods for individual preferences.

References

[1] Jean-Baptiste Alayrac, Jeff Donahue, Pauline Luc, Antoine Miech, Iain Barr, Yana Hasson, Karel Lenc, Arthur Mensch, Katherine Millican, Malcolm Reynolds, et al. Flamingo: a visual language model for few-shot learning. In *NeurIPS*, 2022. 3

[2] Sean Bell, Paul Upchurch, Noah Snavely, and Kavita Bala. Material recognition in the wild with the materials in context database. In *CVPR*, 2015. 4

[3] Sebastian Bosse, Dominique Maniry, Klaus-Robert Müller, Thomas Wiegand, and Wojciech Samek. Deep neural networks for no-reference and full-reference image quality assessment. *IEEE TIP*, 2017. 6, 7

[4] Sebastian Bosse, Dominique Maniry, Klaus-Robert Müller, Thomas Wiegand, and Wojciech Samek. Deep neural networks for no-reference and full-reference image quality assessment. *IEEE TIP*, 2018. 3

[5] Tom Brown, Benjamin Mann, Nick Ryder, Melanie Subbiah, Jared D Kaplan, Prafulla Dhariwal, Arvind Neelakantan, Pranav Shyam, Girish Sastry, Amanda Askell, et al. Language models are few-shot learners. In *NeurIPS*, 2020. 6

[6] Yue Cao, Zhaolin Wan, Dongwei Ren, Zifei Yan, and Wangmeng Zuo. Incorporating semi-supervised and positive-unlabeled learning for boosting full reference image quality assessment. In *CVPR*, 2022. 3

[7] Jun Chen, Han Guo, Kai Yi, Boyang Li, and Mohamed Elhoseiny. Visualgpt: Data-efficient adaptation of pretrained language models for image captioning. In *CVPR*, 2022. 3

[8] Wei-Lin Chiang, Zhuohan Li, Zi Lin, Ying Sheng, Zhanghao Wu, Hao Zhang, Lianmin Zheng, Siyuan Zhuang, Yonghao Zhuang, Joseph E Gonzalez, et al. Vicuna: An open-source chatbot impressing gpt-4 with 90%* chatgpt quality. *https://vicuna.lmsys.org*, 2023. 5, 6, 12, 14

[9] Jacob Devlin, Ming-Wei Chang, Kenton Lee, and Kristina Toutanova. Bert: Pre-training of deep bidirectional transformers for language understanding. *arXiv preprint arXiv:1810.04805*, 2018. 6, 12

[10] Keyan Ding, Kede Ma, Shiqi Wang, and Eero P Simoncelli. Image quality assessment: Unifying structure and texture similarity. *IEEE TPAMI*, 2020. 3, 6, 7

[11] Keyan Ding, Yi Liu, Xueyi Zou, Shiqi Wang, and Kede Ma. Locally adaptive structure and texture similarity for image quality assessment. In *ACM MM*, 2021. 3

[12] Danny Driess, Fei Xia, Mehdi SM Sajjadi, Corey Lynch, Aakanksha Chowdhery, Brian Ichter, Ayzaan Wahid, Jonathan Tompson, Quan Vuong, Tianhe Yu, et al. Palm-e: An embodied multimodal language model. *arXiv preprint arXiv:2303.03378*, 2023. 3

[13] Abhijay Ghildyal and Feng Liu. Shift-tolerant perceptual similarity metric. In *ECCV*, 2022. 3

[14] Tao Gong, Chengqi Lyu, Shilong Zhang, Yudong Wang, Miao Zheng, Qian Zhao, Kuikun Liu, Wenwei Zhang, Ping Luo, and Kai Chen. Multimodal-gpt: A vision and language model for dialogue with humans. *arXiv preprint arXiv:2305.04790*, 2023. 3

[15] Jinjin Gu, Haoming Cai, Haoyu Chen, Xiaoxing Ye, Jimmy Ren, and Chao Dong. Image quality assessment for perceptual image restoration: A new dataset, benchmark and metric. *arXiv preprint arXiv:2011.15002*, 2020. 1, 3

[16] Jinjin Gu, Haoming Cai, Haoyu Chen, Xiaoxing Ye, Jimmy Ren, and Chao Dong. Pipal: a large-scale image quality assessment dataset for perceptual image restoration. *arXiv preprint arXiv:2007.12142*, 2020. 3, 4

[17] Edward J Hu, Phillip Wallis, Zeyuan Allen-Zhu, Yuanzhi Li, Shean Wang, Lu Wang, Weizhu Chen, et al. Lora: Low-rank adaptation of large language models. In *ICLR*, 2021. 5

[18] Shaohan Huang, Li Dong, Wenhui Wang, Yaru Hao, Saksham Singhal, Shuming Ma, Tengchao Lv, Lei Cui, Owais Khan Mohammed, Qiang Liu, et al. Language is not all you need: Aligning perception with language models. *arXiv preprint arXiv:2302.14045*, 2023. 2, 3

[19] Le Kang, Peng Ye, Yi Li, and David Doermann. Convolutional neural networks for no-reference image quality assessment. In *CVPR*, 2014. 3

[20] Junjie Ke, Qifei Wang, Yilin Wang, Peyman Milanfar, and Feng Yang. Musiq: Multi-scale image quality transformer. In *CVPR*, 2021. 3

[21] Taku Kudo and John Richardson. Sentencepiece: A simple and language independent subword tokenizer and detokenizer for neural text processing. In *Proceedings of the 2018 Conference on Empirical Methods in Natural Language Processing: System Demonstrations*, 2018. 5

[22] Bo Li, Yuanhan Zhang, Liangyu Chen, Jinghao Wang, Jingkang Yang, and Ziwei Liu. Otter: A multi-modal model with in-context instruction tuning. *arXiv preprint arXiv:2305.03726*, 2023. 3

[23] Junnan Li, Dongxu Li, Silvio Savarese, and Steven Hoi. Blip-2: Bootstrapping language-image pre-training with frozen image encoders and large language models. *arXiv preprint arXiv:2301.12597*, 2023. 3

[24] Haotian Liu, Chunyuan Li, Qingyang Wu, and Yong Jae Lee. Visual instruction tuning. *arXiv preprint arXiv:2304.08485*, 2023. 2, 3, 5, 6, 7, 14

[25] Xialei Liu, Joost van de Weijer, and Andrew D. Bagdanov. RankIQA: Learning from rankings for no-reference image quality assessment. In *ICCV*, 2017. 3

[26] Chao Ma, Chih-Yuan Yang, Xiaokang Yang, and Ming-Hsuan Yang. Learning a no-reference quality metric for single-image super-resolution. *Computer Vision and Image Understanding*, 2017. 3

[27] Anish Mittal, Anush Krishna Moorthy, and Alan Conrad Bovik. No-reference image quality assessment in the spatial domain. *IEEE TIP*, 2012.

[28] Anish Mittal, Rajiv Soundararajan, and Alan C. Bovik. Making a "completely blind" image quality analyzer. *IEEE Sign. Process. Letters*, 2013.

[29] Anish Mittal, Anush Krishna Moorthy, and Alan Conrad Bovik. No-reference image quality assessment in the spatial domain. *IEEE TIP*, 2022.

[30] Anush Krishna Moorthy and Alan Conrad Bovik. A two-step framework for constructing blind image quality indices. *IEEE Sign. Process. Letters*, 2010.

[31] Anush Krishna Moorthy and Alan Conrad Bovik. Blind image quality assessment: From natural scene statistics to perceptual quality. *IEEE TIP*, 2011. 3

[32] Openai. Gpt-4 technical report. *arXiv preprint arXiv:2303.08774*, 2023. 2, 3, 4, 11

[33] OpenAI. GPT-4V(ision) system card. *https://openai.com/research/gpt-4v-system-card*, 2023. 2, 3, 7, 15

[34] Long Ouyang, Jeffrey Wu, Xu Jiang, Diogo Almeida, Carroll Wainwright, Pamela Mishkin, Chong Zhang, Sandhini Agarwal, Katarina Slama, Alex Ray, et al. Training language models to follow instructions with human feedback. In *NeurIPS*, 2022. 4, 5

[35] Da Pan, Ping Shi, Ming Hou, Zefeng Ying, Sizhe Fu, and Yuan Zhang. Blind predicting similar quality map for image quality assessment. In *CVPR*, 2018. 3

[36] Nikolay Ponomarenko, Vladimir Lukin, Alexander Zelensky, Karen Egiazarian, Marco Carli, and Federica Battisti. Tid2008-a database for evaluation of full-reference visual quality assessment metrics. *Advances of modern radioelectronics*, 2009. 2

[37] Nikolay Ponomarenko, Lina Jin, Oleg Ieremeiev, Vladimir Lukin, Karen Egiazarian, Jaakko Astola, Benoit Vozel, Kacem Chehdi, Marco Carli, Federica Battisti, et al. Image database tid2013: Peculiarities, results and perspectives. *Signal processing: Image communication*, 2015. 3

[38] Ekta Prashnani, Hong Cai, Yasamin Mostofi, and Pradeep Sen. Pieapp: Perceptual image-error assessment through pairwise preference. In *CVPR*, 2018. 1, 2, 3, 6, 7

[39] Alec Radford, Jong Wook Kim, Chris Hallacy, Aditya Ramesh, Gabriel Goh, Sandhini Agarwal, Girish Sastry, Amanda Askell, Pamela Mishkin, Jack Clark, et al. Learning transferable visual models from natural language supervision. In *ICML*, 2021. 5, 12

[40] Michele A Saad, Alan C Bovik, and Christophe Charrier. Blind image quality assessment: A natural scene statistics approach in the dct domain. *IEEE TIP*, 2012. 3

[41] Hamid R Sheikh and Alan C Bovik. Image information and visual quality. *IEEE TIP*, 2006. 2, 6, 7

[42] Shaolin Su, Qingsen Yan, Yu Zhu, Cheng Zhang, Xin Ge, Jinqiu Sun, and Yanning Zhang. Blindly assess image quality in the wild guided by a self-adaptive hyper network. In *CVPR*, 2020. 3

[43] Simen Sun, Tao Yu, Jiahua Xu, Wei Zhou, and Zhibo Chen. GraphIQA: Learning distortion graph representations for blind image quality assessment. *IEEE TMM*, 2022. 3

[44] Huixuan Tang, Neel Joshi, and Ashish Kapoor. Learning a blind measure of perceptual image quality. In *CVPR*, 2011. 3

[45] Hugo Touvron, Thibaut Lavril, Gautier Izacard, Xavier Martinet, Marie-Anne Lachaux, Timothée Lacroix, Baptiste Rozière, Naman Goyal, Eric Hambro, Faisal Azhar, et al. Llama: Open and efficient foundation language models. *arXiv preprint arXiv:2302.13971*, 2023. 2

[46] Hugo Touvron, Louis Martin, Kevin Stone, Peter Albert, Amjad Almahairi, Yasmine Babaei, Nikolay Bashlykov, Soumya Batra, Prajjwal Bhargava, Shruti Bhosale, et al. Llama 2: Open foundation and fine-tuned chat models. *arXiv preprint arXiv:2307.09288*, 2023. 4

[47] Maria Tsimpoukelli, Jacob L Menick, Serkan Cabi, SM Eslami, Oriol Vinyals, and Felix Hill. Multimodal few-shot learning with frozen language models. In *NeurIPS*, 2021. 3

[48] Jianyi Wang, Kelvin CK Chan, and Chen Change Loy. Exploring clip for assessing the look and feel of images. In *AAAI*, 2023. 3

[49] Zhou Wang, Alan C Bovik, Hamid R Sheikh, and Eero P Simoncelli. Image quality assessment: from error visibility to structural similarity. *IEEE TIP*, 2004. 1, 2, 6, 7

[50] Haoning Wu, Zicheng Zhang, Erli Zhang, Chaofeng Chen, Liang Liao, Annan Wang, Chunyi Li, Wenxiu Sun, Qiong Yan, Guangtao Zhai, et al. Q-bench: A benchmark for general-purpose foundation models on low-level vision. *arXiv preprint arXiv:2309.14181*, 2023. 3

[51] Qinghao Ye, Haiyang Xu, Guohai Xu, Jiabo Ye, Ming Yan, Yiyang Zhou, Junyang Wang, Anwen Hu, Pengcheng Shi, Yaya Shi, et al. mplug-owl: Modularization empowers large language models with multimodality. *arXiv preprint arXiv:2304.14178*, 2023. 3

[52] Guanghao Yin, Wei Wang, Zehuan Yuan, Chuchu Han, Wei Ji, Shouqian Sun, and Changhu Wang. Content-variant reference image quality assessment via knowledge distillation. In *AAAI*, 2022. 3

[53] Zhenfei Yin, Jiong Wang, Jianjian Cao, Zhelun Shi, Dingning Liu, Mukai Li, Lu Sheng, Lei Bai, Xiaoshui Huang, Zhiyong Wang, et al. Lamm: Language-assisted multi-modal instruction-tuning dataset, framework, and benchmark. *arXiv preprint arXiv:2306.06687*, 2023. 2, 3, 5, 6, 7, 13

[54] Lin Zhang, Lei Zhang, Xuanqin Mou, and David Zhang. FSIM: A feature similarity index for image quality assessment. *IEEE TIP*, 2011. 2, 6, 7

[55] Richard Zhang, Phillip Isola, Alexei A Efros, Eli Shechtman, and Oliver Wang. The unreasonable effectiveness of deep features as a perceptual metric. In *CVPR*, 2018. 1, 2, 3, 5, 6, 7, 12, 13, 14

[56] Renrui Zhang, Jiaming Han, Aojun Zhou, Xiangfei Hu, Shilin Yan, Pan Lu, Hongsheng Li, Peng Gao, and Yu Qiao. Llama-adapter: Efficient fine-tuning of language models

with zero-init attention. *arXiv preprint arXiv:2303.16199*, 2023. 3

[57] Weixia Zhang, Dingquan Li, Chao Ma, Guangtao Zhai, Xiaokang Yang, and Kede Ma. Continual learning for blind image quality assessment. *IEEE TPAMI*, 2022. 3

[58] Weixia Zhang, Guangtao Zhai, Ying Wei, Xiaokang Yang, and Kede Ma. Blind image quality assessment via vision-language correspondence: A multitask learning perspective. In *CVPR*, 2023. 3

[59] Haozhe Zhao, Zefan Cai, Shuzheng Si, Xiaojian Ma, Kaikai An, Liang Chen, Zixuan Liu, Sheng Wang, Wenjuan Han, and Baobao Chang. Mmicl: Empowering vision-language model with multi-modal in-context learning. *arXiv preprint arXiv:2309.07915*, 2023. 3, 6

[60] Heliang Zheng, Jianlong Fu, Yanhong Zeng, Zheng-Jun Zha, and Jiebo Luo. Learning conditional knowledge distillation for degraded-reference image quality assessment. *ICCV*, 2021. 3

[61] Wei Zhou and Zhou Wang. Quality assessment of image super-resolution: Balancing deterministic and statistical fidelity. In *ACM MM*, 2022. 3

[62] Deyao Zhu, Jun Chen, Xiaoqian Shen, Xiang Li, and Mohamed Elhoseiny. MiniGPT-4: Enhancing vision-language understanding with advanced large language models. *arXiv preprint arXiv:2304.10592*, 2023. 2, 3, 5, 6, 7

[63] Hancheng Zhu, Leida Li, Jinjian Wu, Weisheng Dong, and Guangming Shi. MetaIQA: deep meta-learning for no-reference image quality assessment. In *CVPR*, 2020. 3

Appendix

A. Overview

This *Appendix* is structured as follows. Dataset details are described in Appendix B, followed by the methodology details in Appendix C. Appendix D provides additional ablation studies. More quantitative results, qualitative results, and failure cases are presented in Appendix E.

B. Dataset Details

In this section, we provide additional descriptions and statistics of the introduced M-BAPPS dataset.

In-context learning for response generation. As detailed in the main paper, GPT-4 [32] is employed to convert human-annotated questionnaire options into a natural language paragraph. Yet, GPT-4 tends to produce responses that are overly verbose and potentially misleading. To mitigate this, we supply GPT-4 with two human-written examples to align the generated responses with a consistent writing style. Empirically, in-context learning effectively resolves these issues, yielding high-quality responses.

Questions in the question set. We show various question examples in the qualitative results of Task–1 (*quality description*, Fig. A8 & A9), Task–2 (*quality comparison*, Fig. A10 & A11), and Task–3 (*comparison reasoning*, Fig. A12, A13, & A14). This corroborates that users may express similar questions in different sentences, as discussed in the main paper.

Table A1. **Response length statistics** in our M-BAPPS dataset, reported as word count / string length. † For Task–2's evaluation, only the bi-classification ground-truth is utilized, without the necessity for validation set statistics.

	Task–1 Quality Description	Task–2 Quality Comparison	Task–3 Comparison Reasoning
Train	135.1 / 888.9	19.0 / 131.7	143.3 / 886.4
Validation	143.8 / 947.3	-†	140.0 / 883.3

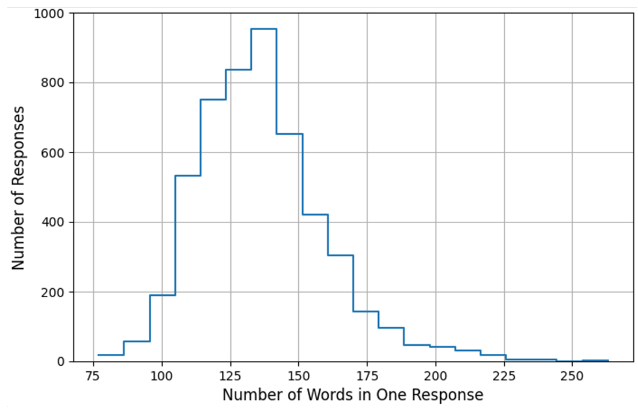

Figure A1. **Distribution of word length** in our M-BAPPS dataset.

Statistics of the response length in our M-BAPPS dataset are illustrated in Tab. A1. We present metrics on both word count and string length. For the evaluation of Task–2 (*quality comparison*), only the bi-classification ground-truth is utilized, so there is no need for statistics of the validation set. The distribution of word length in our M-BAPPS dataset is depicted in Fig. A1.

Statistics of questionnaire options are presented in Fig. A2 and Fig. A3. As detailed in the main paper, when annotating, annotators first complete a carefully designed questionnaire. Here we provide statistical breakdowns of the questionnaire's options. Distortion-related option statistics appear in Fig. A2. Due to the distinct distortion options in Task–1 (*quality description*) and Task–3 (*comparison reasoning*), their counts are presented separately. Texture-related option statistics are outlined in Fig. A3.

Wordcloud of M-BAPPS dataset is depicted in Fig. A4. We manually exclude "Image A" and "Image B" from Fig. A4, as they are constant proper nouns across all texts.

C. Methodology Details

In this section, we describe in detail the setup of model architecture and the calculation of metrics.

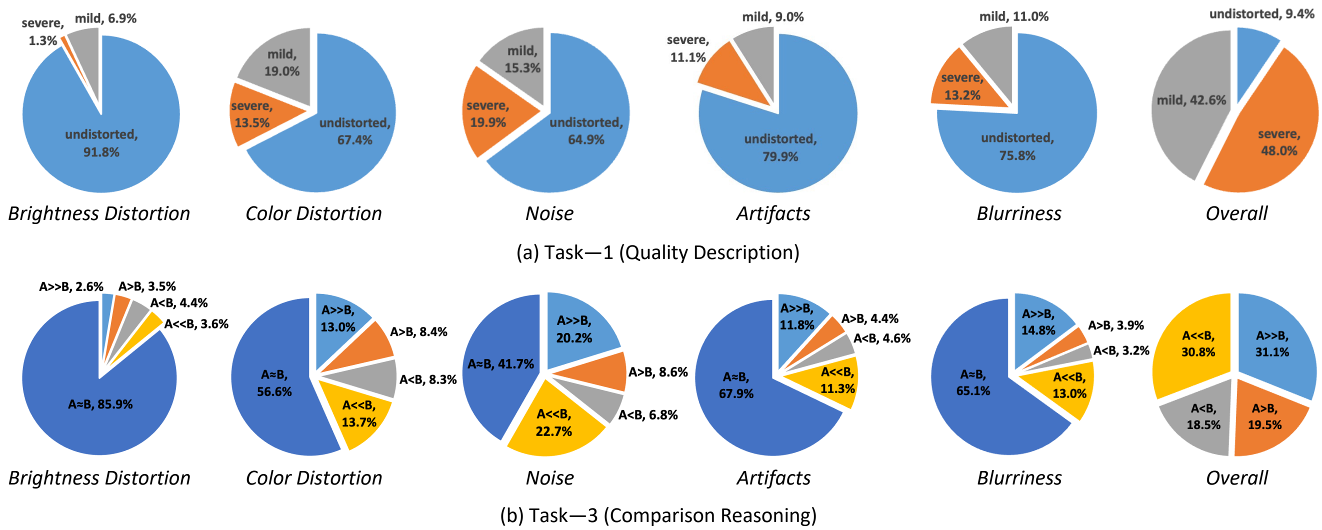

Figure A2. **Statistics of distortion-related options** in the questionnaire with respect to **(a)** Task–1 (*quality description*) and **(b)** Task–3 (*comparison reasoning*). Note that there is no questionnaire for Task–2 (*quality comparison*), hence no statistic is required.

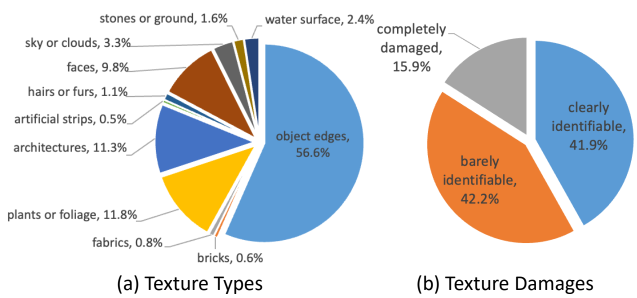

Figure A3. **Statistics of texture-related options** in the questionnaire with respect to **(a)** texture types and **(b)** texture damages.

Figure A4. **Wordcloud** of our M-BAPPS dataset, where “Image A” and “Image B” are manually excluded, since they are proper nouns across all texts.

C.1. Architecture

Model setup. The image size in the BAPPS dataset [55] is 64 × 64, and we pad it to 70 × 70 with zero-padding. Subsequently, we partition the image into 25 patches, with each sized at 14 × 14. We encode the image patches into 25 visual tokens using the CLIP pre-trained ViT-L/14 [39], with each token having the channel of 1024. To accommodate the smaller image size of 70 × 70, as opposed to the standard 224 × 224, we truncate the position embeddings in ViT accordingly. The image projection layer projects these visual tokens to the hidden dimension of the Vicuna-v1.5-7B [8], which is 4096. In LoRA, the rank and scale factor are both set as 16. There are 32 attention layers in Vicuna-v1.5-7B in total. In each attention layer, the projection weights of “query”, “key”, “value”, and “output” are adjusted using two delta parameters with the shape of 4096 × 16 and 16 × 4096, respectively.

C.2. Metrics

Accuracy. We deploy GPT-3.5 to convert varied textual comparison results into binary classification results (*i.e.*, determining whether A or B is better) for accuracy computation. Upon gathering approximately 10k textual comparison results and their binary classifications, we train a BERT [9] model, achieving 97.5% agreement with GPT-3.5 in the test dataset. This model will be made available for those lacking access to GPT-3.5. However, the BERT model is tailored to evaluate the model trained on our data. Its performance on out-of-distribution data is not guaranteed.

GPT4-score. To compute the GPT4-score for one response, we input GPT-4 with the following contents: “context”, “question”, “answer_1”, “answer_2”, and “instruction”. The “instruction” directs GPT-4 to assess two answers (“answer_1” and “answer_2”) to the same “question” using the “context” knowledge, and then rate each answer on a scale of $[0, 10]$. The “context” contains all informa-

Table A2. **Ablation studies regrading LoRA rank** with accuracy metric on BAPPS benchmark [55].

LoRA Rank	8	12	16	24	32
Traditional	77.8	77.1	**78.4**	78.2	77.2
CNN	81.0	81.1	**82.7**	82.3	81.5
Average	79.4	79.1	**80.6**	80.3	79.4

tion in the human-labeled questionnaire, which is the correct knowledge for GPT-4 to evaluate answers. The "question" refers to the quality-related question posed to the MLLMs. The "answer_1" is actually the ground-truth response, which is labeled by human-evaluators. The "answer_2" is the response of the MLLM to be evaluated. Then, the score of "answer_2" (*i.e.*, the MLLM to be evaluated) relevant to "answer_1" (*i.e.*, the ground-truth) serves as the GPT4-score of "answer_2". We calculate the final metric by averaging the scores across all samples. As discussed in the main paper, the GPT4-score tends to be overly generous for low-quality responses, resulting in inflated scores. One example is shown in Fig. A5, where a fully wrong response still receives a GPT4-score of 66.7%.

Reasonable-rate evaluated by humans. Human evaluators are requested to label each response as either reasonable or unreasonable, based on the provided images and corresponding responses. One "reasonable" response should adhere to three criteria. (1) The response must accurately identify the most important quality issue that directly influences the comparison result. (2) The response should avoid serious false positive distortions conflicting with human evaluation. (3) The response's description, reasoning, and conclusion should align closely. Minor errors not violating these three rules are permissible.

D. Ablation Studies

In this section, we conduct more ablation studies to verify the effectiveness of our methodologies.

Influences of LoRA rank are illustrated in Tab. A2. Our DepictQA is insensitive to this hyper-parameter, and the best performance is achieved with the LoRA rank as 16.

Different methods to distinguish multiple images. In addition to the unique tag method introduced in the main paper, we investigate alternative strategies for managing multiple images. (1) Image embedding. We add a trainable embedding to visual tokens for each image type. In *comparison* and *reasoning* tasks, distinct embeddings are assigned to the reference image, Image A, and Image B. For the *description* task, the embeddings for the reference image and Image A are added to the tokens of the reference images and distorted images, respectively. (2) Unique image projector. We utilize unique image projectors for varied image categories. These projectors are specifically initialized for the

Table A3. **Comparison of different methods to distinguish multiple images**. The comparison ability is assessed by accuracy within Traditional / CNN categories. The reasoning ability is evaluated by reasonable-rate. The performance of image embedding and unique projector is obviously inferior to unique tag.

Method	Comparison	Reasoning
Image Embedding	67.0 / 66.9	26.0
Unique Projector	75.1 / 77.2	40.0
Unique Tag	**78.4 / 82.7**	**53.0**

Table A4. **Comparison of global feature and local feature map**. The comparison ability is assessed by accuracy within Traditional / CNN categories. The reasoning ability is evaluated by reasonable-rate. Local feature map surpasses global feature obviously.

	Comparison	Reasoning
Global Feature	76.7 / 80.8	34.0
Local Feature Map	**78.4 / 82.7**	**53.0**

reference image, Image A, and Image B in *comparison* and *reasoning* tasks. In the *description* task, only projectors for the reference image and Image A are employed. The experimental results are illustrated in Tab. A3. The performance of image embedding and unique projector is obviously inferior to unique tag. We suspect that the reason could be that changing the visual tokens differently for various images may confuse the model.

Comparison of global feature and local feature map. The ViT-L/14 image encoder produces a singular global feature token and a multi-token local feature map. Either can function as visual tokens of the MLLM. We analyze the performance differences between the global feature and local feature map in Tab. A4. The global feature demonstrates lesser effectiveness than the local feature map, particularly in reasoning tasks. This disparity might come from the global feature's singular visual token, which restricts the amount of information conveyed.

Impacts of content description data on texture diversity. Incorporating external content description data, specifically the Detailed Description Dataset in [53], stably enhances the performance, as discussed in the main paper. Training with content description data also enriches the diversity of texture types recognized, even beyond the predefined categories in our training set, as depicted in Fig. A6. For instance, in the last two examples in Fig. A6, though the texture types of "trees" and "flowers" are usually annotated as "plants" in the training set, we still correctly predict these fine-grained texture types.

E. More Results

More quantitative results, qualitative results, and failure cases are presented in this section.

Reference Image

Image A

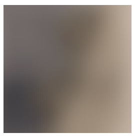

Image B

Context (human-labeled questionnaire): texture type: architecture; texture damage of Image A: clearly identifiable; texture damage of Image B: completely damaged and unidentifiable; brightness distortion : Image A is similar to Image B; color distortion: Image A is similar to Image B; noise: Image A is similar to Image B; artifact: Image A is similar to Image B; ***blurriness: Image A is significantly better than Image B***; ***overall: Image A is better than Image B***.

Answer_1 (human-labeled ground-truth): The quality of ***Image A is significantly superior to that of Image B***. ***Image A outperforms Image B by a large margin in terms of blurriness***. Additionally, both images exhibit comparable performance in terms of brightness distortion, color distortion, noise, and artifacts. More importantly, Image A demonstrates lower overall distortion and exhibits clearly visible architectural textures, whereas the architectural textures in Image B are completely damaged. Therefore, Image A's advantages in terms of blurriness and texture preservation enable it to surpass Image B in overall quality.

Answer_2 (LAMM with LLaMA-2-chat-7B): Based on the analysis, it appears that both Image A and Image B have similar content, but there are some differences in their quality. The brightness of the two images is similar, indicating that the lighting conditions were similar when the images were captured. However, ***the color quality of Image B is considered better than Image A***. The color quality of Image A is described as poor, which could be due to factors such as low contrast, low resolution, or excessive noise. ***The noise in Image A is also considered high***, which can make the image appear blurry or distorted. On the other hand, Image B has a higher color quality and a lower noise level, which results in a sharper and more detailed image.

Scoring and reasoning of GPT-4: ***9.0 for Assistant 1 and 6.0 for Assistant 2***. Assistant 1 provided a more accurate and detailed response, closely following the context provided by the user. They correctly identified the differences in texture damage and blurriness, and acknowledged the similarities in brightness distortion, color distortion, noise, and artifacts. Assistant 2, on the other hand, made some incorrect assumptions about the color quality and noise levels, which were not mentioned in the context. Assistant 1's response was more helpful, relevant, and precise, while Assistant 2's response was less accurate and detailed.

GPT4-score of Answer_2 is 6.0 / 9.0 = **66.7%**

Figure A5. **GPT4-score sometimes exhibits excessive confidence in low-quality responses**, though widely adopted as metrics in MLLMs [8, 24]. In this case, a fully wrong response still receives a GPT4-score of 66.7%.

	Texture Type			
Image	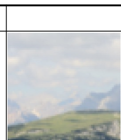			
Prediction	Mountains †	Jeans †	Trees †	Flowers †
Closest Annotation in Training Set	Ground	Fabrics	Plants	Plants

† Beyond our pre-defined texture types in training set

Figure A6. **Training with the content description data improves the diversity of texture types in responses**, which even beyond our pre-defined texture types in training set.

E.1. More Results of Quality Description

Qualitative results of quality description are illustrated in Fig. A8 and A9. We sample these results from:

- Different distortions. *e.g.*, *blurriness* in A8a & A9c, *noise* in A8c & A9e, *color distortion* in A8d & A9d.
- Various contents. *e.g.*, *plants* in A8c & A8e, *architectures* in A8d & A9b, *people* in A8f.
- Diverse distortion degrees. *e.g.*, *severe* in A8a & A9d, *mild* in A8b, A8d, & A8e, *no distortion* in A8f & A9b.

E.2. More Results of Quality Comparison

Consistency with the tendencies of human annotators. The ground-truth scores in the BAPPS dataset [55] represent the proportion of annotators favoring Image B. In the validation set of BAPPS, there are 5 annotators in total, so the value of the ground-truth score varies across [0, 0.2, 0.4, 0.6, 0.8, 1.0]. As shown in Tab. A5, when we exclude the samples with high label uncertainty in the BAPPS dataset, the comparison accuracy of our DepictQA improves significantly, indicating that our model behaves consistently with the tendencies of human annotators.

Table A5. **Our DepictQA behaves consistently with the tendencies of human annotators**. When excluding samples with high label uncertainty in BAPPS dataset [55], the comparison accuracy improves significantly.

Excluded Labels	$\emptyset$	$\{0.4, 0.6\}$	$\{0.2, 0.4, 0.6, 0.8\}$
Traditional	78.4	84.7	90.2
CNN	82.7	88.4	93.3
Average	80.6	86.6	91.8

Qualitative results of quality comparison are illustrated in Fig. A10 and A11. DepictQA aligns closely with human judgments under the circumstances of:

- Different types of distortions. *e.g.*, *blurriness* in A11b & A11c, *noise* in A10a & A10b, *color distortion* in A10g & A11f, *artifacts* in A11a & A11d.
- Different texture types. *e.g.*, architectures in A10a & A11c, *object edges* in A11f, *water surface* in A10b & A10f, *plants* in A10d & A11d.
- Both images suffering from severe distortions. *e.g.*, *color distortion* in A & *blurriness* in B in A10d, *noise* in A & *blurriness* in B in A11c.

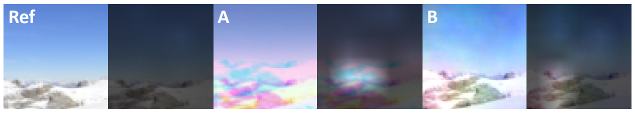

... The quality of Image B is significantly superior to that of Image A. Image A noticeably falls short in two key factors, ***color distortion and artifacts*** ...

Figure A7. **Visualization of the attention map**. We visualize decoder attention weights between the **highlighted words** and the visual tokens. Our model focuses on relevant regions containing text-described distortions.

E.3. More Results of Comparison Reasoning

Qualitative results of comparison reasoning are illustrated in Fig. A12, A13, and A14. Similar to Appendix E.2, these samples are sampled from:

- Various categories of distortions. *e.g.*, *color distortion* in A12a & A12c, *blurriness* in A13c & A14a, *artifacts* in A14b & A14c, *noise* in A13a & A14d.
- Different image contents. *e.g.*, *sky and clouds* in A12b, *architectures* in A13a & A14c, *plants* in A12d & A13c.
- Both images with severe distortions. *e.g.*, *color distortion* in A & *blurriness* in B in A14a, *color distortion* in A & *noise* in B in A12c.

E.4. Failure Cases

Failure cases of DepictQA in *quality description* and *comparison reasoning* tasks are presented in Fig. A15. (1) Fig. A15a and A15b show DepictQA incorrectly identifying distortion types, leading to wrong quality assessments in the quality description task. (2) In Fig. A15c, DepictQA mistakenly attributes the noise in Image A to Image B, resulting in an incorrect comparison result. As reflected in Fig. 4 in the main paper, the unique tag approach does not completely resolve the confusion issue. (3) In Fig. A15d, DepictQA fails to recognize an unusual distortion (*i.e.*, complete semantic content washout in Image B). This is primarily due to the absence of such distortions in the training set.

E.5. More Results of GPT-4V

Qualitative results of GPT-4V [33] in *comparison reasoning* task are shown in Fig. A16. GPT-4V gives quite detailed comparison reasoning results, which is the main reason for its excellent GPT4-score (see Tab. 4 in the main paper).

Failure cases of GPT-4V in *comparison reasoning* task are given in Fig. A17. Despite GPT-4V providing detailed reasoning texts, it mistakenly describes distortions, texture damages, and comparison results.

E.6. Extension

Potential to localize distorted regions. In Fig. A7, we visualize decoder attention weights between the texts that describe distortions and the visual tokens. Our model focuses on relevant regions containing text-described distortions. This invites our future research into precise distortion localization based on textual outputs.

Reference: 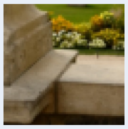 Image: 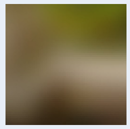 ,

What criteria are you using to assess the overall quality of the image, and can you explain your assessment in detail?

The overall quality of this image is severely compromised, primarily due to the issue of blurriness. Although the distortions in brightness, color, noise, and artifacts are minimal, the problem of blurriness significantly reduces the overall clarity of the image. Moreover, the texture features of the image are completely damaged, making it impossible to discern the texture information originally contained in the image. Therefore, it can be concluded that blurriness is the main reason for the decline in the overall quality and texture damage of this image.

(a)

Reference:  Image: 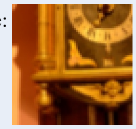 ,

How would you rate the quality of the image, and what specific elements contribute to your assessment?

The quality of this image is quite good, with only minor issues. The brightness and color are well-balanced, and there are no significant noise or artifacts, indicating a high level of image quality. However, the image's clarity is slightly reduced, possibly due to blurring, which impacts the overall quality of the image to a certain extent. Overall, the image distortion is minimal, and the texture features, especially the texture of the object edges, can still be clearly identified. Therefore, the image quality is generally good, with the main issue being the slight blurring, which may impact the image's clarity, but not severely.

(b)

Reference: 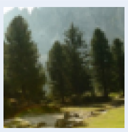 Image: 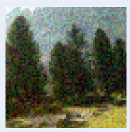 ,

Could you please analyze the quality of the image, and then elaborate on your assessment?

The overall quality of this image is severely compromised, primarily due to the significant noise within the image, which drastically reduces its clarity and results in poor visual effects. Although there are no apparent distortions in brightness and color, and the degree of artifacts and blurring remains at a low level, these factors cannot offset the damage that noise has done to the image quality. Additionally, the damage to the image's texture is also severe, particularly the texture of the plants, which is now entirely unrecognizable, demonstrating the destructive impact of noise on image quality. Therefore, it can be definitively concluded that the quality of this image is severely affected, with noise being the primary factor leading to this outcome.

(c)

Reference: 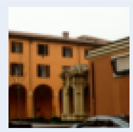 Image: 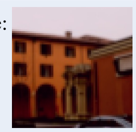 ,

In your opinion, what are the strengths and weaknesses of the image in terms of quality, and why?

The overall quality of this image is good, with only minor distortions. Among the five evaluation factors, brightness, noise, artifacts, and blurring have virtually no distortion, indicating that the image's brightness, clarity, authenticity, and sharpness are well preserved. However, there is a certain degree of distortion in terms of color. Nevertheless, due to the good performance of the other factors, the overall distortion of the image is still considered minor. In terms of texture, the texture of architecture is clearly visible and is not greatly affected by color distortion. Therefore, I conclude that despite minor color distortion, the overall quality and texture quality of this image still remain at a high level.

(d)

Reference: 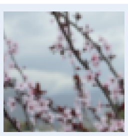 Image: 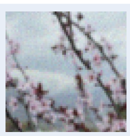 ,

Assess the image's quality with a critical eye, highlighting both strengths and areas for improvement.

The overall quality of this image is acceptable, but there are some issues related to blur and noise. Although the distortion in terms of brightness, color, and artifacts is minimal, the slight blur and noise have somewhat impacted the image quality. This is also reflected in the evaluation of overall distortion, where the overall distortion level of this image is slightly higher than that of the reference image. Moreover, the blur and noise have somewhat impacted the recognition of the plant texture. The degree of texture damage is barely recognizable. Overall, although the image quality is acceptable, the slight blur and noise have impacted the image texture, resulting in a certain degree of loss in image quality.

(e)

Reference: 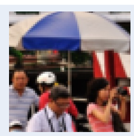 Image:  ,

Evaluate the overall quality of the image and provide a comprehensive explanation of your assessment.

The image has excellent performance in terms of quality assessment, with hardly any noticeable distortion. The level of distortion is minimal, nearly negligible, indicating that the image quality is high and nearly perfect. The texture features of the image are also well preserved, with the facial texture clearly visible, and the degree of texture damage is extremely low. This suggests that the image has been created using advanced image processing technology, with virtually no artifacts, and the processing is done quite effectively. Overall, the image has high quality, with almost no distortion, especially in terms of texture, where the original features are well preserved, making it an outstanding image.

(f)

Figure A8. **Qualitative results of our DepictQA on quality description task**. Our DepictQA could clearly identify distortions and texture damages, then weigh the impacts of various aspects to draw the final conclusion.

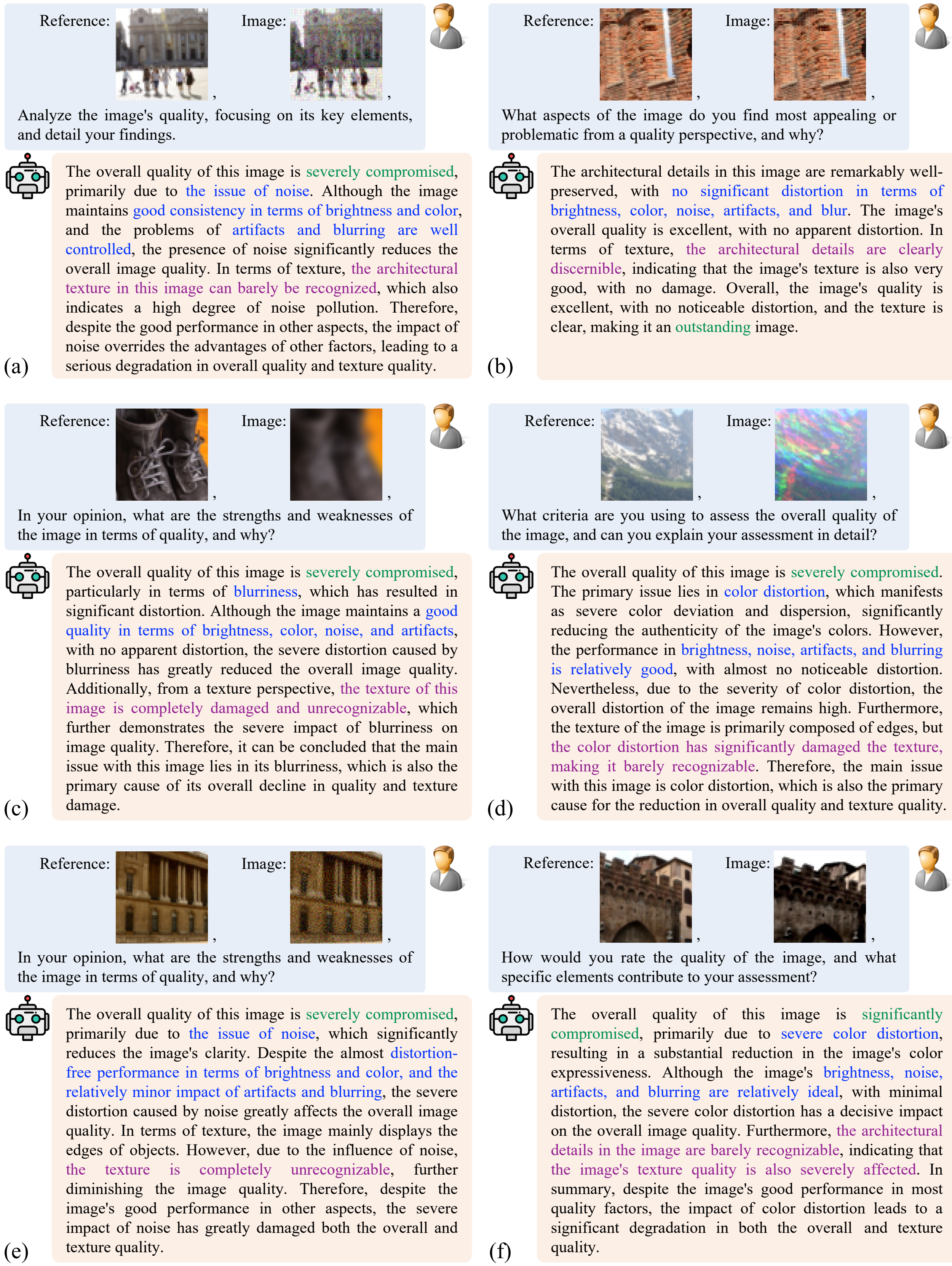

Figure A9. **Qualitative results of our DepictQA on quality description task**. Our DepictQA could clearly identify distortions and texture damages, then weigh the impacts of various aspects to draw the final conclusion.

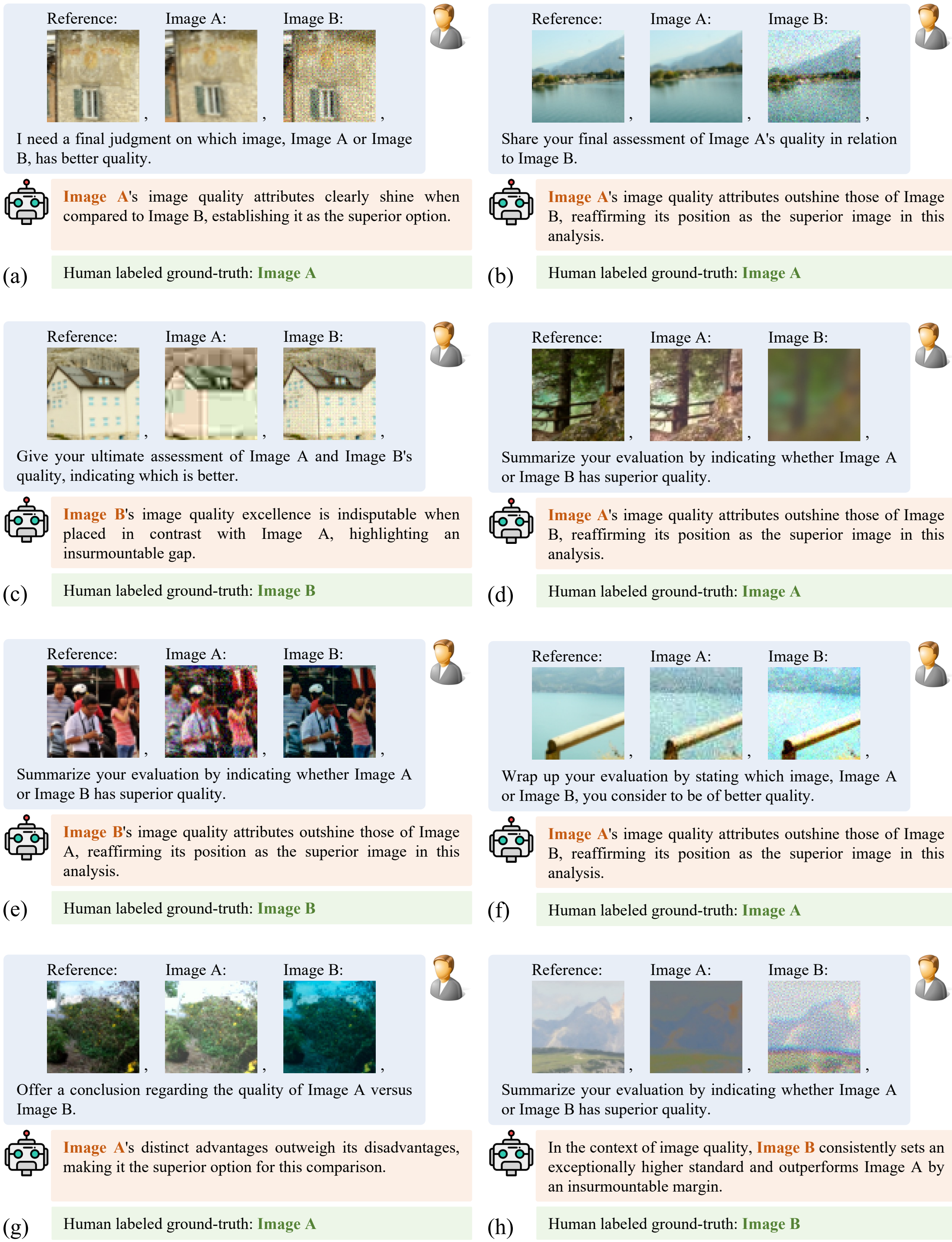

Figure A10. **Qualitative results of our DepictQA on quality comparison task**. Our DepictQA aligns quite well with human judgments.

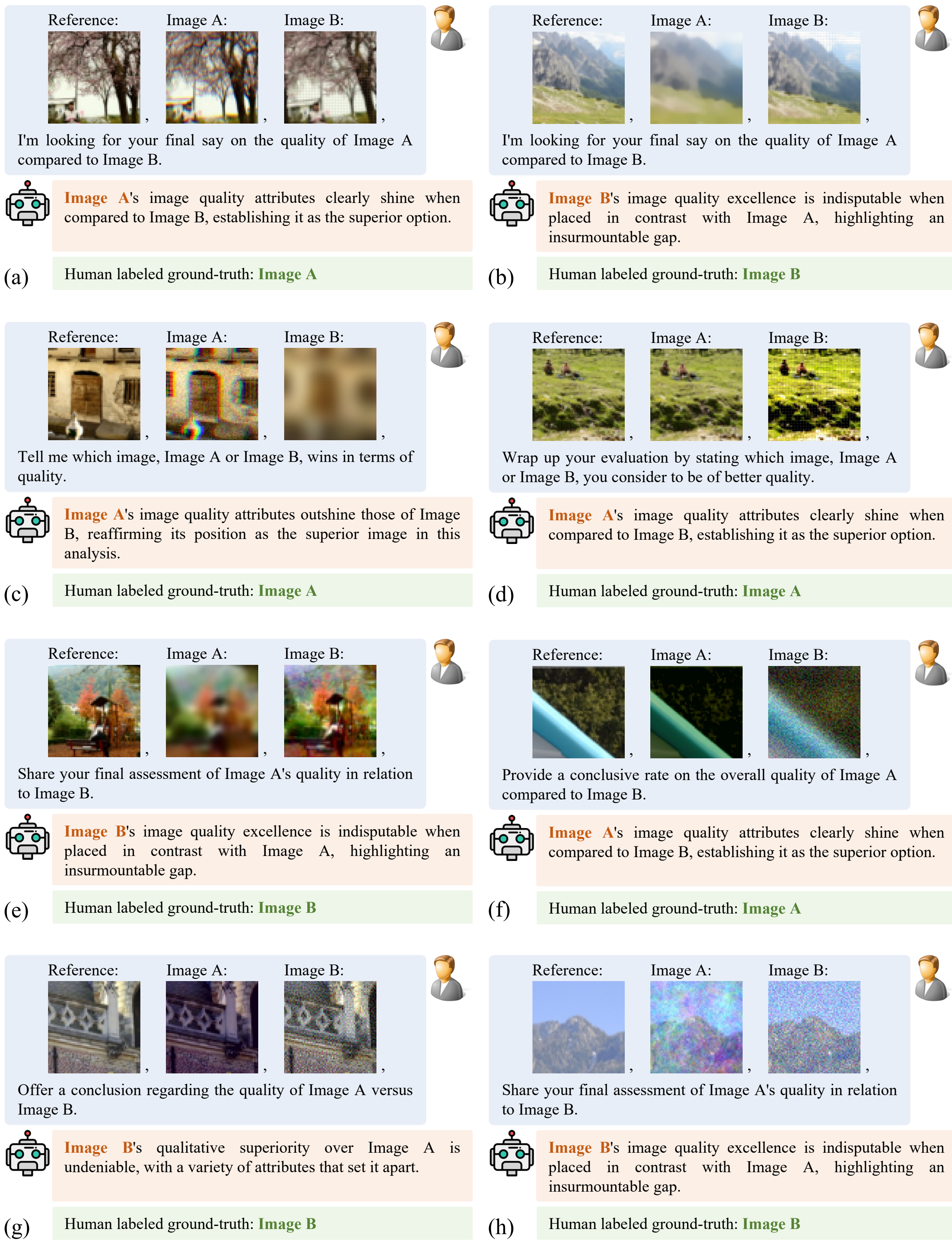

Figure A11. **Qualitative results of our DepictQA on quality comparison task**. Our DepictQA aligns quite well with human judgments.

Figure A12. **Qualitative results of our DepictQA on comparison reasoning task**. Our DepictQA could comparatively identify distortions, then weigh the impacts of these distortions to the texture damages, and finally draw the final comparison conclusion.

Figure A13. **Qualitative results of our DepictQA on comparison reasoning task**. Our DepictQA could comparatively identify distortions, then weigh the impacts of these distortions to the texture damages, and finally draw the final comparison conclusion.

Figure A14. **Qualitative results of our DepictQA on comparison reasoning task**. Our DepictQA could comparatively identify distortions, then weigh the impacts of these distortions to the texture damages, and finally draw the final comparison conclusion.

Reference: Image:

What criteria are you using to assess the overall quality of the image, and can you explain your assessment in detail?

The overall quality of this image is significantly compromised, primarily due to the noise issue within the image. Although the brightness and color representation are almost undistorted, and the degree of artifacts and blurring can be largely disregarded, the severe distortion caused by the noise has greatly impacted the overall image quality. Moreover, the recognizability of the texture is also reduced, with only the texture along the object edges being barely discernible. Therefore, it can be clearly stated that noise is the main culprit behind the overall degradation of this image, particularly the reduction in texture quality.

(a)

Reference: Image:

Could you please analyze the quality of the image, and then elaborate on your assessment?

The overall quality of this image is relatively good, but there is a slight deviation in color representation, resulting in minor color distortion. However, this does not significantly impact the overall image quality. Concurrently, the image maintains a good quality in terms of brightness, noise, artifacts, and blurring, with almost no distortion, which contributes to the preservation of image clarity and color. Despite the slight color distortion, it does not cause much damage to the texture of the architecture, and I can still clearly identify the texture of the architecture.

(b)

Reference: Image A: Image B:

Which image has a better quality, Image A or Image B? Can you explain the comparison result with detailed factors?

I find that both images exhibit similar levels of brightness distortion and color distortion. However, Image A outperforms Image B in terms of noise handling, but is slightly inferior in dealing with artifacts effects. Both images demonstrate comparable performance in terms of blurriness. Overall, the total distortion level of Image A is slightly lower than that of Image B. Despite this, both images excel in the handling of texture, with facial textures and object textures being clearly identifiable. Therefore, I conclude that the quality of Image A is slightly superior to that of Image B. Although Image A is somewhat inferior in terms of artifacts handling, its advantage in noise handling results in a lower overall distortion level, thereby enhancing the overall quality of the image. As for the texture quality, both images perform well, with no significant differences in identification. Thus, considering all factors, the quality of Image A is better.

(c)

Reference: Image A: Image B:

Could you please analyze the quality of both Image A and Image B and then elaborate on your findings regarding their differences in quality?

We found that both exhibited similar performance in terms of brightness distortion and color distortion. However, Image A significantly underperformed Image B in terms of noise, which had a substantial impact on the overall quality of Image A. Conversely, Image A outperformed Image B in terms of artifacts, but Image B held an advantage in terms of blurriness. Overall, the total distortion of Image A was slightly worse than that of Image B. In terms of texture degradation, both Image A and Image B were barely recognizable, which may have been caused by noise and blurriness. Despite Image A's superior performance in artifacts, the impact of noise resulted in its overall and texture quality being slightly inferior to that of Image B. Therefore, considering all factors, the quality of Image B is superior to that of Image A.

(d)

Figure A15. **Failure cases of DepictQA** in **(a)(b)** quality description task and **(c)(d)** comparison reasoning task.

Reference: Image A: Image B:

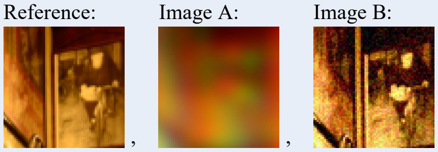

Compare the overall quality of Image A with Image B and provide a comprehensive explanation for your comparison.

Upon meticulously analyzing Image A and Image B against the pristine backdrop of the Reference Image, the ensuing insights are delineated:

Brightness and Exposure: Image A presents an overwhelming dominance of warm, fiery colors, which makes discerning any specific details nearly insurmountable. In stark contrast, Image B provides a better balance in its exposure, revealing more detailed facets of the scene, aligning closer to the brighter and clearer ambiance of the Reference Image.

Color Representation: Image A is awash with intense, saturated warm hues that obliterate any distinct differentiation in the scene's elements. Image B, while still on the warmer spectrum, manages to exhibit more nuanced color gradations, making it more akin to the golden tones captured in the Reference Image.

Noise and Clarity: Image A suffers from an overwhelming haze, making the image grainy and significantly compromising its clarity. Image B, despite having some level of graininess, offers a clearer view, with details more discernible and aligning better with the clarity depicted in the Reference Image.

Texture and Sharpness: Due to the intense saturation and possible over-enhancement of Image A, it's challenging to gauge the textures. Image B, while not as crisp as the Reference Image, does a commendable job of presenting textures—especially of the wooden elements and the person therein—more palpably.

Artifacts and Distortions: Image A is marred by apparent over-processing, leading to artifacts and potential data loss. Image B, though a touch grainy, retains more authentic details, making it more congruent with the fidelity of the Reference Image.

Blurriness: Image A's overwhelming saturation renders any evaluation of its blurriness challenging. Image B, while not pin-sharp, certainly boasts better focus and detail preservation, mirroring the Reference Image's clarity more faithfully.

To encapsulate, Image A, awash with overpowering hues and artifacts, diverges dramatically from the Reference Image's clarity and authenticity. Image B, despite its minor imperfections, closely emulates the Reference Image's overall quality, detail representation, and color palette. Consequently, when juxtaposed, the quality of Image B substantially outperforms that of Image A.

(a)

Reference: Image A: Image B:

Compare the overall quality of Image A with Image B and provide a comprehensive explanation for your comparison.

In conducting a comprehensive comparison of the quality between Image A and Image B with respect to the Reference Image, the following detailed evaluation can be made:

Starting with color distortion, Image A displays prominent color discrepancies, with hues that appear overly vibrant and unrealistic when juxtaposed with the Reference Image. This leads to a loss of realness and a departure from the natural appearance. Image B, on the other hand, although still demonstrating minor deviations from the true colors, portrays a more accurate color representation, closely aligning with the Reference Image.

When examining the factor of noise, Image A is severely hampered by the presence of excessive noise, especially in the shadow regions, compromising its clarity and overall appearance. Image B, while also exhibiting some level of noise, does so to a much lesser extent, maintaining a cleaner and clearer visual experience more akin to the Reference Image.

Regarding brightness, Image A seems to lean towards a heightened brightness level, causing some details, especially in well-lit areas, to be washed out. Image B achieves a more balanced brightness, ensuring both shadow and light regions are adequately depicted, more closely mirroring the Reference Image.

In terms of texture clarity, Image A's texture appears significantly degraded, particularly observable in areas like the arch of the bridge, rendering it almost unrecognizable. Image B, while not perfectly capturing the texture from the Reference Image, manages to retain a commendable level of texture detail, making elements like the bridge's stone structure discernible.

Artifacts are another area of concern in Image A, where certain sections seem pixelated, suggesting possible compression or encoding issues. Image B, in contrast, offers a smoother appearance with minimal artifacts, providing a visual experience that's closer to the Reference Image.

In conclusion, by examining the factors such as color fidelity, noise, brightness, texture clarity, and the prevalence of artifacts, it becomes evident that Image B's quality is notably superior to that of Image A. While neither image flawlessly replicates the Reference Image, Image B certainly stands as the more commendable representation in terms of overall quality when compared to Image A.

(b)

Figure A16. **Qualitative results of GPT-4V** in comparison reasoning task.

Reference: 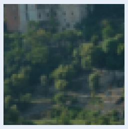, Image A: 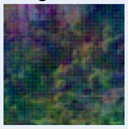, Image B: 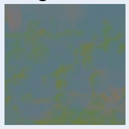,

Compare the overall quality of Image A with Image B and provide a comprehensive explanation for your comparison.

In comparing the quality of Image A and Image B, using the provided high-quality reference image as a benchmark, the following observations arise:

The quality of Image A is substantially compromised in comparison to Image B. Primarily, the color fidelity in Image A is significantly distorted, with hues taking on an unnatural, pixelated gradient. Image B, while not perfect, exhibits colors that are more consistent and closely align with the reference image, especially in the sky region which appears cleaner and more natural.

Regarding brightness, Image A is much darker and lacks proper luminance balance. This obscurity diminishes the clarity of elements such as the trees and the architectural structures. Image B, however, showcases a better adaptation to the reference image in terms of brightness, with areas like the sky and trees being more discernible.

Noise is a glaring issue in Image A. The excessive graininess and pixel irregularities, particularly in the tree line and the structures, considerably deteriorate its quality. Image B stands out with a comparatively smoother texture, although slight noise can be detected, it remains closer to the reference image's clarity.

Considering artifacts, Image A is replete with them, especially noticeable in the sky and around the architectural details. Image B, while not devoid of artifacts, has fewer of them, and they are less disruptive to the overall scene, making it more aligned with the reference.

Sharpness is another differentiator. The details in Image A are blurry, lacking in crispness, particularly around the trees and architectural elements. Image B manages to capture clearer outlines and details, especially in the distant structures, rendering it more in sync with the clarity of the reference image.

In terms of texture, Image A's are heavily degraded, especially in the foliage and architectural structures, which appear smudged and unrecognizable. Image B, although not achieving the high fidelity of the reference image, manages to retain a decent level of texture, particularly in the tree leaves and the distant buildings.

Conclusively, while both Image A and Image B have their limitations, Image B substantially outperforms Image A in multiple facets, including color accuracy, brightness, noise reduction, artifact minimization, sharpness, and texture quality. Aligning these findings with the reference image, it's evident that the quality of Image B is notably superior to that of Image A.

(a)

Reference: 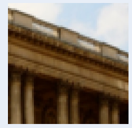, Image A: 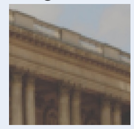, Image B: 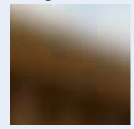,

Compare the overall quality of Image A with Image B and provide a comprehensive explanation for your comparison.

In the analysis of Image A and Image B against the Reference Image, the differences in quality become clear through the following examination:

The quality of Image A is notably inferior when juxtaposed with Image B. Beginning with clarity, Image A exhibits an evident blurriness that considerably reduces the visibility of the architectural details in the image. The iconic pillars and the facade, which seem to be integral parts of a classical structure, lack sharpness in Image A. This obscurity, in turn, diminishes the viewer's ability to clearly discern finer details and appreciate the grandeur of the structure.

Contrastingly, Image B showcases these architectural elements with more clarity and precision. The pillars stand out with greater sharpness, and the intricate carvings on the facade are more discernible. The level of detail in Image B aligns more closely with the Reference Image, providing a truer representation of the monument.

In terms of color fidelity, Image A appears washed out with muted tones, failing to capture the richness and depth of the colors observed in the Reference Image. Image B, meanwhile, offers a better color balance, with the golden hues of the structure and the clear blue sky closely mirroring the Reference Image. The gradient of the sky in Image B, transitioning from a deeper blue at the top to a lighter shade near the horizon, provides a naturalistic portrayal.

In terms of texture damages, Image A's blurriness severely impacts texture representation. The intricacies of the stone carvings and the surface details of the structure are lost. Image B, while not fully capturing the texture detail present in the Reference Image, does a commendable job in highlighting the ruggedness and unique patterns of the stone.

Artifacts are minimal in both Image A and Image B. However, Image A's diminished clarity can be perceived as an artifact in itself, significantly affecting the overall viewing experience.

In summation, when the factors of clarity, color representation, texture detail, and overall fidelity to the Reference Image are considered, Image B undeniably offers a superior quality. It provides a clearer, more vibrant, and detailed rendition of the architectural marvel, making it a more accurate visual representation than the blurred and desaturated Image A.

(b)

Figure A17. **Failure cases of GPT-4V** in comparison reasoning task.